Open Access **Baghdad Science Journal** **P-ISSN: 2078-8665**
Published Online First: March, 2023 **2023, 20(5 Suppl.): 1919-1925** **E-ISSN: 2411-7986**

DOI: https://dx.doi.org/10.21123/bsj.2023.7428

Quantum Theory of Atom in Molecules Investigation Trinuclear Ruthenium: DFT Approach

Manal Abed Mohammed

Department of Basic Medical Science, College of Dentistry, University of Kerbala, Kerbala, Iraq.
E-mails address manal.abdmuhammed@uokerbala.edu.iq

Received 15/3/2022, Revised 25/9/2022, Accepted 26/9/2022, Published Online First 20/3/2023, Published 28/10/2023

Abstract:

The topological indices of the "[(μ3-2, 5-dioxyocyclohexylidene)-bis ((2-hydrido)-nonacarbonyl-triruthenium]" were studied within the quantum theory of atoms in the molecule (QTAIM), clusters are analyzed using the density functional theory (DFT). The estimated topological variables accord with prior descriptions of comparable transition metal complexes. The Quantum Theory of Atom, in molecules investigation of the bridging core component, Ru3H2, revealed critical binding points (chemical bonding) between Ru (1) and Ru (2) and Ru (3). Consequently, delocalization index for this non-bonding interaction was calculated in the core of Ru3H2, the interaction is of the (5centre–5electron) class.

Keywords: Aim program, DFT, Delocalization, Laplacian, Ru cluster.

Introduction:

Polynuclear metal clusters represent a large category of coordination combinations with plentiful applications in catalysis. The organometallic catalysis mononuclear and polynuclear clusters may be implemented in homogeneous solution [1]. The major objective of the fields is the inspection of the new strategies to develop catalytic [2]. The electrical structures of low valent transition metal clusters receive a lot of attention [3,4] due to their importance as catalysts in industries and the atypical nature of metal-metal bonds, which are still unexplained to several extent [5,6]. A variety of experimental charge density experiments on M-M bonded compounds have been conducted in response to this interest [7,8].

The powerful method for studying chemical bonding that employs topological evaluation of electron density in this setting of QTAIM [9], analyses on systems that contain lighter atoms (transition metals in the periodic table) have resulted in critical investigations of bonding types and topological electron density characteristics [10]. M-M bonds in transition metals have taken the topic of many experimental and theoretical researches to get deeper information about it such as the reactivity and physical properties like (M-M bond distances, magnetic properties, ionizations, electronic transitions, and redox potential).

Because of the chiral nature of Triruthenium clusters, it is important to use Ruthenium metal clusters as a catalyst. For example, that it is used as a catalyst precursor in the hydrogenation of unsaturated substrate asymmetrical isomers. Therefore this type of cluster under study in many researches[11 -12].

Cabeza and et al., used QTAIM within AIM to investigate N-heterocyclic carbene ligand (MeImCH) face - capping in Triruthenium Clusters $[Ru_3(\mu\text{-}H)_2(\mu_3\text{-}MeImCH)(CO)_9]$[13]. In 1997, Hsiu-Fu Hsu et al., studied some structural properties for big Triruthenium ligand $[Ru3(CO)_9\}x(m_3\text{-}\eta 2\ ,\ \eta\ 2\ ,\ \eta\ 2\text{-}C_{70})]$ (x = 1, 2)[14]. Muhsen Al-Ibadi and his coworkers studied the nature M-M bond for this type of clusters [3,15,16].

This paper reported QTAIM topological investigation for the electron density of di hydride Triruthenium clusters [(μ3-2, 5-dioxyocyclohexylidene)-bis(μ2-hydrido)-nonacarbonyl-triruthenium] to study the properties the nature of M-M, M-H and M-C bonds. Also, studying the delocalization index for the bond order of these bonds[17], a trinuclear cluster that is closed and has twin hydride-bridged carbon and oxygen atoms, as well as a face-capping binding with Ru-C and RuO interactions Fig. 1. As a result, it is possible to compare the topological features of comparable and

different atom-atom bonding within the same molecule, such as the hydride-bridge Ru-H against Ru-C and Ru-Ru contact. These clusters are selected because of no previous QTAIM researches. Also, allowing a better comparisons of different topological properties between two M-M interactions, such as Ru-Ru bonds, H-bridged and ligand-unbridged Ru-Ru interactions.

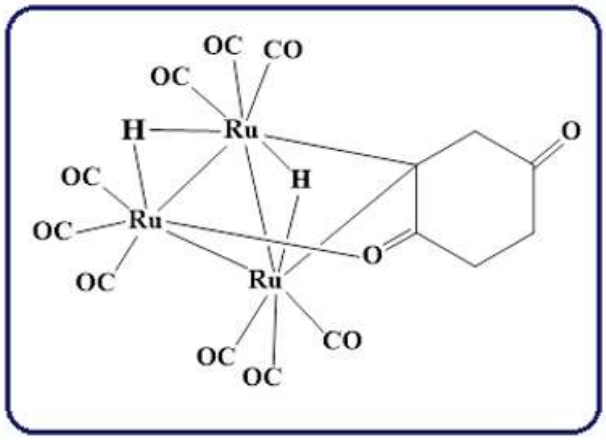

Figure 1. structure of [(μ3-2, 5-dioxyocyclohexylidene)-bis (μ2-hydrido)-nonacarbonyl- Triruthenium].

Computational Methods

Via GAUSSIAN09[18], the electronic structure of a chemical was computed using a computer based on both the experimental (X-ray diffraction data) and theoretically optimal structure. These calculations were carried out using density functional theory " DFT ". The hybrid PBE1PBE functional was evaluated [19]. The 6-31G (p, d) basis set was used for all-electron C, H, and O atoms used the basis sets LanL2DZ for checking the Ruthenium atoms. WTBS (Huzinaga et al.) for Ru atoms and 3-21G (p, d) basis set for other atoms for AIM investigations [20]. The ground state was estimated by electronic wave functions, that is optimized, which used then for AIM topological theoretical computations of (ED) by AIM2000 package [21]. The precision for the integrated features is set at 1.0×10^{-4} (for Laplacian integral electron density) as well as the accuracy for the local features is given at 1.0×10^{-10} that used the gradient of charge density for points critical bonds.

Discussion and Conclusions:

1. Topological Electron Density Properties

The integral collection of the bond critical points (BCP; (3, 1)) is defined by two negative curves (maximum) and one positive curve (minimum), as well as ring critical points (RCP; (3, +1)). With two positive curves and one negative curvature. Bond pathways (BP) are the lines of greatest electron density that connect two interacting atoms. Cage critical point (CCP) has the form (3,+3) within the AIM paradigm[22–24]. A molecular graph is defined as the topology gradient of bonds and ring critical points, as well as the line that connecting between the atoms [25,26]. The complex's molecular graph picture is presented in Fig. 2. BCP values were determined for the Ru-C (10 BCP), Ru-H (2 BCP), C-O (9 BCP), and Ru-O (1 BCP) bonds. The BCP likewise discovered atoms of Ru (1) and Ru (3) and between the Ru (1), Ru (2) and Ru (3). There are no critical points and bond paths. Four RCPs were definitely recognized in the structure, corresponding to the Ru(2)-H(1)-Ru(1)-Ru(3)-H(2), Ru(3)-C(2)-H(2)-Ru(2), Ru(1)-O(1)-C(1)-C(2)-Ru(3), and cyclohexylidene rings. A gradient trajectory map in the Ru (1)-Ru (2)-Ru (3) plane depicts the QTAIM analysis Fig. 3 .The total electron density indicates the BCPs and bp across Ru (1)-Ru (3)-H (2)-Ru (2), along with atomic basins with all atoms on same surface. The results showed that bp's and bcp's connect H (1) and Ru (1).

The total electron density difference trajectory map in the O (1)-Ru (1)-H (1) plane showed that not only bp's, bcp's, and rcp's linked to ring, but also bp's, bcp's of Ru(1) to the RuOC ligand C (1) atoms and Ru(3) interactions with Ru-CC ligand C(2)C(1) atoms as shown in Fig. 4 **.** Furthermore, Ru (1) and Ru (3) include a Trans to O - CO ligand (1). The cyclohexylidene plane has the hydride H (1), but it not bonded to any of the plane's atoms.

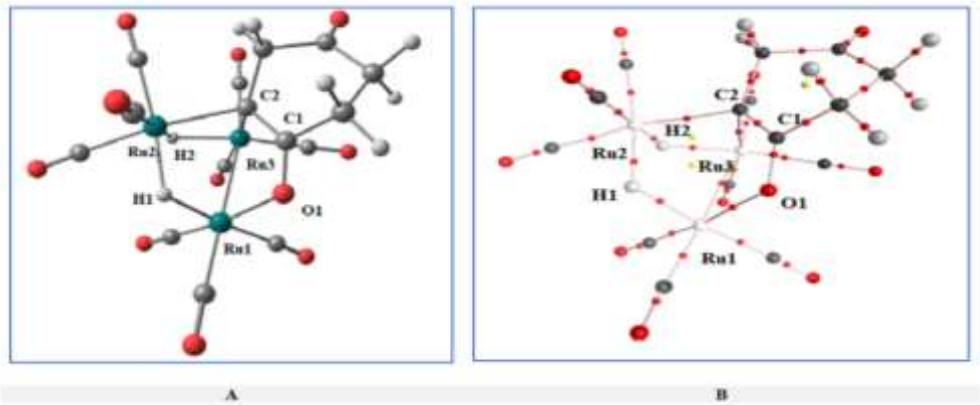

Figure 2. (A) Structure optimization of [(μ3-2, 5-dioxyocyclohexylidene)-bis (μ2-hydrido)-nonacarbonyl-triruthenium]. (B) The molecular graphs of the complex, with straight lines denoting bond paths and bright red and yellow circles denoting bond and ring critical locations, respectively.

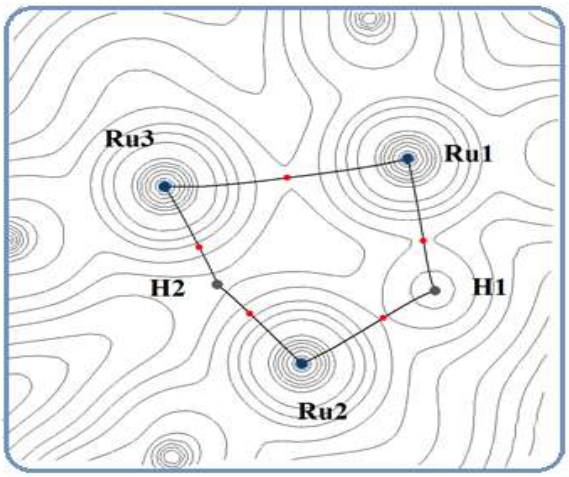

Figure 3. Graph indicates the total ED of atoms in the Ru (1)-Ru (2)-Ru (3) plane, bond paths (black path), bcps (red dots), and an RCP are displayed (yellow dots)

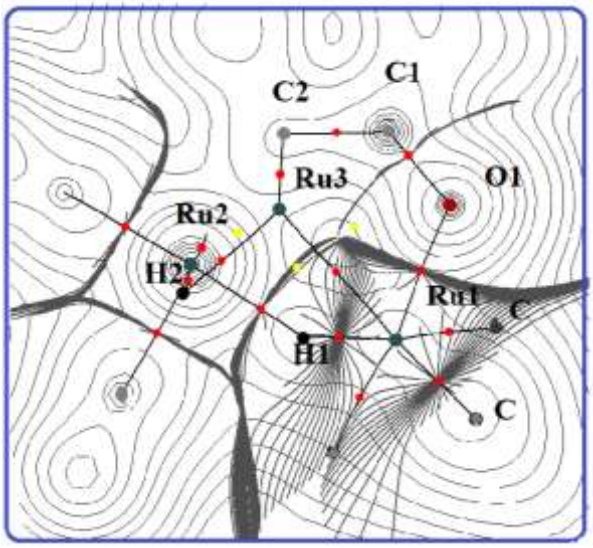

Figure 4. Total ED of atoms in the O (1)-Ru (1)-H (1) plane, bond paths (black path), bcps (red dots), and an RCP are displayed (yellow dots).

The QTAIM used Bader's strategy [10] as shown in Table. 1 uses charge density analysis to examine atom bonding. This method of topological analysis proposes reducing difference between the theoretical results and the experimental ones in calculations of charge density, ρ(r). Moreover, it is also Laplacian, $\nabla^2\rho(r)$, H(r) G(r), V(r), and H(r), total energetic densities and the kinetic energy for the combination under investigation[27], all of them show the difference respectively .

The charge density concentration towards atomic interaction lines $\nabla^2\rho b < 0$. This concentration of charge minimizing Orthogonality of ρb in the bond interaction and reduce the potential energy. While the $\nabla^2\rho b > 0$ denotes that the electrons density is concentrated towards each nucleus [28]. To distinguish any interaction as covalent or ionic and into closed-shell versus open-shell by the sign of Laplacian can be better characterized by H(r) = G(r) +V(r) [29]. This formula is the balance between the kinetic G(r) and V(r) detects the nature of bonding(3). The sign of $\nabla^2\rho b$ and the sign of H(r), respectively. Pure closed-shell interactions are indicated when both $\nabla^2\rho(b)$ and H(r) are positive; transit closed-shell interactions are indicated when both$\nabla^2\rho(b)$ and H(r) are negative; and pure shared shell interactions are indicated when both $\nabla^2\rho(b)$ and H(r) are negative.[30,31].

As a result of our analysis for the electron density (ED) for cluster under study, we observed that, basing on the facts on its topological and energetic local features, the metal-metal bond and the hydride H bridge Ru-H are classed as Pure closed-shell interactions between covalent bonds. Both C_1-C_2 and Ru-O bonds are transit closed-shell connections, because they have opposite charges for $\nabla^2\rho b$ and H(r). The low values of ρ_{BCP} are similar to those for an ionic bond, but the negative $\mathbf{H_{BCP}}$ agrees with a covalent contribution[32].

The charge distribution was measured by the bond ellipticities (εr_b). Results showed high magnitude for Ru (n)-H (8.78, 8.400, 5.564 and 9.347) for all bonds and the average bonds ellipticities of Ru-CO while the magnitude of Ru-Ru and Ru-C have low value. This difference is according to the electronegativity of the atoms[33].

Table 1. Topological parameters of the cluster's bonds critical points, electron densities, Laplacian of the electron densities ($\nabla^2\rho$), kinetic energy densities (Gr_b), potential energy densities (Vr_b), total energy densities (Hr_b), and ellipticities (εr_b), (εr_b).decolazation index δ(A, B).

Bond	ρr_b(e$A^{\circ -3}$)	$\nabla^2{}_{\rho rb}$(e$A^{\circ -5}$)	Gr_b(he^{-1})	Hr_b (he^{-1})	Vr_b (he^{-1})	εr_b	δ(A, B)
Ru_1-Ru_3	0.0412	0.0510	0.0205	0.0075	0.0281	1.2290	0.3890
Ru_1-H_1	0.0827	0.2320	0.0807	0.0223	0.0223	8.7850	0.4340
Ru_2-H_1	0.0782	0.2560	0.0790	0.0193	0.0991	5.5640	0.6760
Ru_2-H_2	0.0768	0.2390	0.0782	0.0183	0.0966	8.4000	0.3600
Ru_3-H_2	0.0759	0.2310	0.0760	0.0182	0.0943	9.3470	0.4100
Ru_1-O_1	0.0640	0.4450	0.1038	-0.0070	0.0960	6.5650	0.3600
Ru_3-C_2	0.0833	0.3120	0.9640	0.0181	0.1146	2.6970	0.5280
Ru_2-C_2	0.0845	0.3190	-0.0982	0.0183	0.1160	2.1390	0.5300
Ru-CO*	0.1340	0.5290	0.1810	0.0940	0.2300	6.0010	1.0900
C_1-O_1	0.3570	0.3060	0.6443	0.5670	1.2120	3.9990	0.9630
C_1-C_2	0.2980	-0.7120	0.1032	0.2810	0.3850	2.0340	1.0890

Figure 5 a graph of the Laplacian of the charge densities estimated to planes containing Ru1-Ru2-Ru3, which is very relevant for analysing Ru-Ru and Ru-H bonds. Because of their pseudo-octahedral coordination, the valence shell charge depletion (VSCD) of all Ru atoms results in a perfect cubic form in the cluster[34,35].

Furthermore, a valence shell charge concentration (VSCCs) for hydro as bridge atoms is oriented toward the Ru atoms.

The result of the absence of a bond path with critical points in the shape of the Laplacian distribution among Ru(1)-Ru(2) and Ru(2)-Ru(3)atoms indicated that there was no bonding electron pairs between these transition metal atoms[36]. The map shows the unavailability of a critical bond point and the disappearance of a bond line in the form of the Laplacian distribution of the middle Ru(1)-Ru(2) and Ru(2)-Ru(3) atoms ,so no bonding between these transition metal atoms is found .

The delocalization index has been calculated for unbridged Ru-Ru, Ru-H, Ru-O and Ru-CO bonds, a resultant of Ru-H delocalization index is 0.47, which is comparable to the value estimated by Cabeza et al. (13) for the Ru–H bonds in the "[Ru3(-H)2(3-MeImCH) (CO)9]" cluster (0.474). Importantly, the obtained statistics are consistent with the few examples expected for M-H interactions. [37]. According to these investigations, the number of electron pairs in the Ru-H bond is a half electron pair.

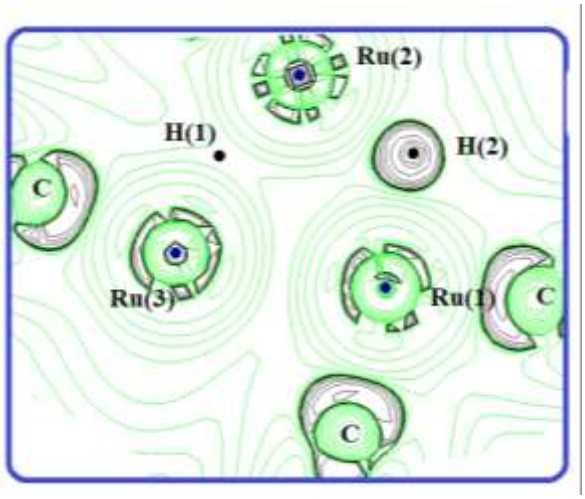

Figure 5. The electron densities inside this cluster's Ru (1)-Ru (2)-Ru (3) planar are represented by a Laplacian graphic.

Table. 1, indicates that the delocalisation index for Ru (1)-Ru (2) Ru (3) bonds is somewhat close, but the topological parameters for these bonds differ significantly. The most important discovery is that when the bonding and non-bonding delocalization indices are summed together, there is number of electron pairs in the Ru (1)-H (1) –Ru (2) –H (2) –Ru (3) core is (2.1). In the bridged core portions, our data suggest a multicentre 5c-5e interaction.

Table. 1, shows the estimated topological features of the Ru-CO bonds, which are consistent with the literature [37]. According to our data, the estimated value of BCP for Ru-CO bonds (0.134Å^{-3}) is substantially higher than for Ru-Ru bonds and lower than the projected value for non-metal atom covalent bonds. The calculated delocalization indices were used to demonstrate the existence of -

back bonding in Metal-CO interactions owing to -back donating, which includes the M...CO interaction.

The Ru (2,3) ...C (1) and Ru (1) ...O (1) delocalization indices were computed in the same way as the Ru-CO calculations to indicate the existence or absence of bonding. As seen in Table 1, Ru is a pure -donor with no -bonding characteristic.

Conclusions:

Topological indices produced from the QTAIM analysis are used to investigate the interactions in the triruthenium "[(μ3-2, 5-dioxyocyclohexylidene)-bis (2-hydrido)-nonacarbonyl-triruthenium]" cluster that is important in catalyst industrials and not found in the theoretical study for this compound. The AIM studies of the bridging core component Ru_3H show that the Ru (1)...Ru (2) and Ru (2)...Ru (3) interaction lacks a BCPs and bond bp s. According to our estimates, because of their pseudo-octahedral coordination, the valence shell charge depletion (VSCD) of all Ru atoms results in a perfect cubic form in the cluster and the bridged core part is a 5c–5e type. AIM studies of the estimated topological indices of dioxyocyclohexylidene ligand indicate a significant degree of -electron delocalization within the ligand ring.

Author's declaration:

- Conflicts of Interest: None.
- I hereby confirm that all the Figures and Tables in the manuscript are mine. Besides, the Figures and images, which are not mine, have been given the permission for re-publication attached with the manuscript.
- Ethical Clearance: The project was approved by the local ethical committee in University of Kerbala, Iraq.

References:

1. Nielsen MT, Padilla R, Nielsen M. Homogeneous Catalysis by Organometallic Polynuclear Clusters. Clust Sci. 2019; 3, 456-463.
2. Dikhtiarenko A, Khainakov S, Gimeno J. Mixed-valence μ3-oxo-centered triruthenium cluster $[Ru_3^{(II,III,III)}(\mu_3\text{-}O)(\mu\text{-}CH_3CO_2)_6(H_2O)_3]\cdot 2H_2O$: Synthesis, structural characterization, valence-state delocalization and catalytic behavior. Inorganica Chim Acta. 2017; 107-116, https://dx.doi.org/10.1016/j.ica.2016.05.046 .
3. Al-Ibadi MA, Taha A, Hasan Duraid AH, Alkanabi T. A theoretical investigation on chemical bonding of the bridged hydride triruthenium cluster: [Ru3 (μ-H)(μ3-κ2-hamphox-N,N)(CO)9]. Baghdad Sci J. 2020; 17(2): 488–493, https://dx.doi.org/10.21123/bsj.2020.17.2.0488 .
4. Helal SR, Al-Ibadi MAM, Hasan AH, Taha A. The QTAIM Approach to Chemical Bonding in Triruthenium Carbonyl Cluster: [Ru3 (μ-H)(μ 3-κ 2-Haminox-N,N)(CO)9]. Phys Conf Ser. 2018; 1032(1). https://dx.doi.org/10.1088/1742-6596/1032/1/012068
5. FB B, Lewis J, Road L. The Triruthenium Cluster Anion $[Ru_3H(CO)_{11}]^-$: Preparation, Structure, and Fluxionality. J Chem Soc Dalton trans. 1979; 76(1356): 1356–1361. https://doi.org/10.1039/DT9790001356 .
6. Kameo H, Ito Y, Shimogawa R, Koizumi A, Chikamori H, Fujimoto J , et al. Synthesis and Characterisation of Tetranuclear Ruthenium Polyhydrido Clusters with Pseudo-Tetrahedral Geometry. Dalton Trans. 2017; 77:6-11. https://dx.doi.org/10.1039/C6DT04523E .
7. Shimogawa R, Tsurumaki Y, Suzuki H, Takao T. Selective Synthesis of a Triruthenium Pentahydrido Complex with Mixed-Cp Ligands C 5. Organometallics. 2019; 3 :345-354, https://dx.doi.org/10.1021/acs.organomet.9b00503 .
8. Heijser W, Baerends EJ, Ros P. Electronic Structure of Binuclear Metal Carbonyl Complexes Diatomic metals and metallic clusters. Faraday Symp. Chem. Soc; 1979; 211-234. https://doi.org/10.1039/FS9801400211 .
9. Bader RFW. Atoms in Molecules. Acc Chem Res. 1985;9–15. doi:10.1002/0470845015.caa012.
10. Bader RFW. A Quantum Theory of Molecular Structure and Its Applications. Chem. Rev.. 1991;91(5):893–928, https://dx.doi.org/10.1021/cr00005a013 .
11. Briard P, Cabeza JA, Llamazares A, Ouahab, L, and Riera V.. Synthesis and Structural Characterization of Triruthenium Cluster Complexes Containing Bridging Vl-Phenyl and Terminal Vl-Phenyl Ligands Arising from the Cleavage of Triphenylphosphine Ligands. Organometallics. 1993; 12:1006–1008.
12. Cabeza JA, Franco RJ, Llamazares A, Riera V, Prez-carreiio E, Van Der Maelen JF. η^1-Aryl-Bridged Triruthenium Cluster Complexes. Organometallics. 1994;77(12):55–59.
13. Cabeza JA, F J, Maelen VD, Granda SG. Topological Analysis of the Electron Density in the N-Heterocyclic Carbene Triruthenium Cluster $[Ru_3(\mu\text{-}H)2(\mu3\text{-}MeImCH)(CO)_9]$ (Me2Im = 1,3-dimethylimidazol-2-ylidene). Organometallics , 2009; 28(13): 3666–3672, https://dx.doi.org/10.1021/om9000617 .
14. Hsu H, Wilson SR, Shapley JR. Triruthenium cluster complexes of C70. Synthesis and structural characterization of {Ru3(CO)9}x(μ3-η^2, η^2, η^2-C70)] (x = 1, 2). Chem Commun. 1997:1125–1126.
15. Al-ibadi MAM. QTAIM Analysis of the Bonding in Pyridyl- N- Heterocyclic Carbene Triruthenium carbonyl cluster: [Ru3(μ-H)(μ-κ3C2,N-pyCH2 ImMe) (CO)9] (ImMe=3-methylimidazol-2- ylidene). J Univ Babylon Pure Appl Sci. 2018; 26(6): 322–335.
16. Al-Kanabi D T O, Al-ibadi MAM, Mohammed H J. Theoretical topological analysis of the electron density in Picolyl N-Heterocyclic Carbene Triruthenium carbonyl cluster. J Kufa Chem Sci. 2014; 3(9): 1–14.
17. Pelayo-vázquez JB, González-bravo FJ, Leyva MA,

Rosales-hoz MJ. Reactivity of 1 . 4-benzoquinone with trinuclear ruthenium and osmium clusters : Facile hydrogenation of the quinoid fragment. J Organmet. Chem. 2016; 812c : 207-216
18. MacDonald B, Ranjan P, Chipman H. GPfit: An R Package for Fitting a Gaussian Process Model to Deterministic Simulator Outputs. Stat. Softw. 2015; 64(12): A1-23. https://dx.doi.org/10.18637/jss.v064.i12.
19. Huzinaga S, Klobukowski M. Well-tempered Gaussian basis sets for the calculation of matrix Hartree-Fock wavefunctions. Chem Phys Lett. 1993; 212(3-4): 260-264.
20. Huzinaga S, Miguel B. A comparison of the geometrical sequence formula and the well-tempered formulas for generating GTO basis orbital exponents. Chem Phys Lett. 1990;175(4):289–291. https://dx.doi.org/10.1016/0009-2614(90)80112-Q .
21. Biegler-Konig F, Schonbohm J. Update of the AIM2000-Program for atoms in molecules Comput Chem. 2002; 23(15): 1489-1494. https://dx.doi.org/10.1002/jcc.10085 .
22. Nakanishi W, Hayashi S, Narahara K. Atoms-in-molecules dual parameter analysis of weak to strong interactions: Behaviors of electronic energy densities versus Laplacian of electron densities at bond critical points. Phys Chem A. 2008;112(51):13593–13599. https://dx.doi.org/10.1021/jp8054763 .
23. Grimme S. Theoretical bond and strain energies of molecules derived from properties of the charge density at bond critical points. J Am Chem Soc. 1996; 118(6): 1529–1534. https://dx.doi.org/10.1021/ja9532751 .
24. Bader RFW. A bond path: a universal indicator of bonded interactions. J Phys Chem A. 1998; 102(37): 7314–7323.
25. Gatti C. Chemical Bonding in Crystals: new dirrections. Cryst Mater. 2005; 220(5-6): 399-457.
26. Bader RFW. Atoms in Molecules. Acc Chem Res. 1985; 18(1): 9-15. https://dx.doi.org/10.1021/ar00109a003.
27. Matta CF. On the connections between the quantum theory of atoms in molecules (QTAIM) and density functional theory (DFT): a letter from Richard F. W. Bader to Lou Massa. Struct Chem. 2017; 28(5): 1591-1597. https://doi.org/10.1007/s11224-017-0946-7
28. Guisasola EB ,Gutiérrez LJ, Salcedo RE, Garibotto FM, Andujar SA, Enriz RD, et al. Conformational transition of Aβ42 inhibited by a mimetic peptide. A molecular modeling study using QM/MM calculations and QTAIM analysis. Comput Theor Chem. 2016;1080:56–65, https://dx.doi.org/10.1016/j.comptc.2016.02.002 .
29. Espinosa E, Alkorta I, Rozas I, Elguero J, Molins E. About the evaluation of the local kinetic, potential and total energy densities in closed-shell interactions. Chem Phys Lett. 2001; 336(5-6): 457–461, https://dx.doi.org/10.1016/S0009-2614(01)00178-6 .
30. LaPointe SM, Farrag S, Bohórquez HJ, Boyd RJ. QTAIM study of an α-helix hydrogen bond network. J Phys Chem B. 2009; 113(31): 10957–10964, https://dx.doi.org/10.1021/jp903635h .
31. Moosavi M, Banazadeh N, Torkzadeh M. Structure and Dynamics in Amino Acid Choline-Based Ionic Liquids: A Combined QTAIM, NCI, DFT, and Molecular Dynamics Study. J Phys Chem B. 2019; 123(18): 4070–4084, https://dx.doi.org/10.1021/acs.jpcb.9b01799 .
32. Macchi P, Sironi A. Chemical bonding in transition metal carbonyl clusters: Complementary analysis of theoretical and experimental electron densities. Coord Chem Rev. 2003; 238–239: 383–412, https://dx.doi.org/10.1016/S0010-8545(02)00252-7 .
33. Razooqi MS, Al-ani HN. Quantum Mechanical Calculations and Electrochemical Study of Vibrational Frequencies, Energies in Some Flavonoids molecules. Iraqi J Sci. 2022; 63(6): 2331–2344. https://dx.doi.org/10.24996/ijs.2022.63.6.2 .
34. Al-kirbasee NE, Raheem S, Alhimidi H, Al-ibadi MAM. QTAIM study of the bonding in triosmium trihydride cluster. Baghdad J Sci. 2021; 18(4): 1279–1285.
35. Ridha AR, Abbas ZM. Theoretical study of density distributions and size radii of 8B and 17Ne. Iraqi J Sci. 2018; 59(2): 1046–1056, https://dx.doi.org/10.24996/IJS.2018.59.2C.8 .
36. Gervasio G, Bianchi R, Marabello D. About the topological classification of the metal-metal bond. Chem Phys Lett. 2004; 387(4–6): 481–484, https://dx.doi.org/10.1016/j.cplett.2004.02.043 .
37. Macchi P, Donghi D, Sironi A. The Electron Density of Bridging Hydrides Observed via via Experimental and Theoretical Investigations on $[Cr_2(\mu_2\text{-}H)(CO)_{10}]^-$. J Am Chem Soc. 2005; 127(47): 16494–16504.

Open Access **Baghdad Science Journal** **P-ISSN: 2078-8665**
Published Online First: March, 2023 **2023, 20(5 Suppl.): 1919-1925** **E-ISSN: 2411-7986**

استخدام QTAIM لتشخيص مركب للروثينيوم ثلاثي النوى

منال عبد محمد

قسم العلوم الطبية الاساسية، كلية طب الاسنان، جامعة كربلاء، كربلاء، العراق.

الخلاصة:

الدراسات الطوبولوجية لـمركب "[μ3-2 ،5-dioxyocyclohexylidene) -bis ((2-hydrido) -nonacarbonyl-triruthenium]" باستخدام نظرية QTAIM (نظرية الكم للذرات في الجزيئات) تم تشخيص المركب ضمن مستوىDFT حيث تتفق المتغيرات الطوبولوجية المقدرة مع الدراسات السابقة للمعقدات المعدنية الانتقالية المماثلة حيث أظهرت الدراسة لمكون الجسر الأساسي Ru3H2 وجود النقاط الحرجة للرابطة بين الذرات Ru(1), Ru(2),Ru(3) ونتيجة لتلك الدراسة تم حساب مؤشر عدم التمركز لها الترابط الكيميائي الخاص بمركز المعقد حيث وجد ان نوع الترابط هو 5C-5e .

الكلمات المفتاحية: برنامج AIM ، دالة الكثافة، عدم التمركز، لا بلاسين، روثينيوم كلوستر.